

See discussions, stats, and author profiles for this publication at: <https://www.researchgate.net/publication/262147811>

# Improved Multifrequency Phase-Modulation Method That Uses Rectangular-Wave Signals to Increase Accuracy in Luminescence Spectroscopy

ARTICLE in ANALYTICAL CHEMISTRY · MAY 2014

Impact Factor: 5.64 · DOI: 10.1021/ac4030895 · Source: PubMed

CITATIONS

4

READS

51

9 AUTHORS, INCLUDING:



**Santiago Medina Rodríguez**

University of Granada

23 PUBLICATIONS 48 CITATIONS

SEE PROFILE



**Francisco J. Arregui**

Universidad Pública de Navarra

296 PUBLICATIONS 3,494 CITATIONS

SEE PROFILE



**Jorge F Fernandez-Sanchez**

University of Granada

77 PUBLICATIONS 867 CITATIONS

SEE PROFILE



**Alberto Fernández-Gutiérrez**

University of Granada

407 PUBLICATIONS 6,247 CITATIONS

SEE PROFILE

# Improved Multifrequency Phase-Modulation Method That Uses Rectangular-Wave Signals to Increase Accuracy in Luminescence Spectroscopy

Santiago Medina-Rodríguez,<sup>†,‡</sup> Ángel de la Torre-Vega,<sup>\*,†</sup> Francisco J. Sainz-Gonzalo,<sup>‡</sup> Marta Marín-Suárez,<sup>‡</sup> César Elosúa,<sup>§</sup> Francisco J. Arregui,<sup>§</sup> Ignacio R. Matias,<sup>§</sup> Jorge F. Fernández-Sánchez,<sup>\*,‡</sup> and Alberto Fernández-Gutiérrez<sup>‡</sup>

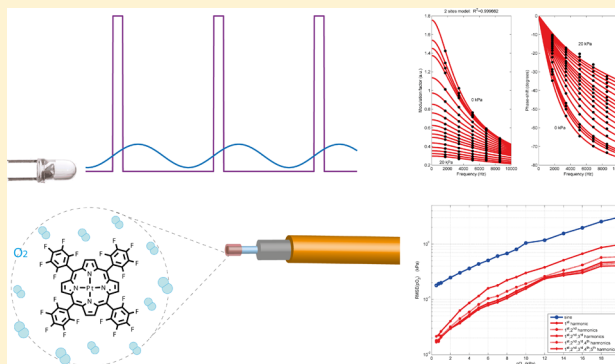
<sup>†</sup>Department of Signal Theory, Networking and Communications, Information and Communication Technologies Research Centre, University of Granada, C/Periodista Rafael Gómez 2, E-18071 Granada, Spain

<sup>‡</sup>Department of Analytical Chemistry, Faculty of Sciences, University of Granada, Avda. Fuentenueva s/n, E-18071 Granada, Spain

<sup>§</sup>Department of Electrical and Electronic Engineering, Arrosadia Campus, Public University of Navarre, E-31006 Pamplona, Spain

## S Supporting Information

**ABSTRACT:** We propose a novel multifrequency phase-modulation method for luminescence spectroscopy that uses a rectangular-wave modulated excitation source with a short duty cycle. It is used for obtaining more detailed information about the luminescence system: the information provided by different harmonics allows estimating a model for describing the global frequency response of the luminescent system for a wide range of analyte concentration and frequencies. Additionally, the proposed method improves the accuracy in determination of the analyte concentration. This improvement is based on a simple algorithm that combines multifrequency information provided by the different harmonics of the rectangular-wave signal, which can be easily implemented in existing photoluminescence instruments by replacing the excitation light source (short duty cycle rectangular signal instead of sinusoidal signal) and performing appropriate digital signal processing after the transducer (implemented in software). These claims have been demonstrated by using a well-known oxygen-sensing film coated at the end of an optical fiber [a Pt(II) porphyrin immobilized in polystyrene]. These experimental results show that use of the proposed multifrequency phase-modulation method (1) provides adequate modeling of the global response of the luminescent system ( $R^2 > 0.9996$ ) and (2) decreases the root-mean-square error in analytical determination (from 0.1627 to 0.0128 kPa at 0.5 kPa  $O_2$  and from 0.9393 to 0.1532 kPa at 20 kPa  $O_2$ ) in comparison with a conventional phase-modulation method based on a sinusoidally modulated excitation source (under equal luminous power conditions).



Lifetime measurements are preferred in luminescence spectroscopy since they are less susceptible to errors than intensity measurements.<sup>1–3</sup> The luminescent lifetime can be determined by methods that proceed either in the time domain (pulsed methods) or in the frequency domain (phase-modulation methods).<sup>1,4</sup> Pulsed measurements are ideally suited for elimination of background luminescence and scattering, but they require expensive and complex instrumentation (such as high-speed photodetectors) and high computational cost.<sup>1,2,5</sup> On the other hand, lifetime phase-modulation measurements do not require sophisticated instrumentation<sup>6,7</sup> and allow the use of simple and cheap light sources and electronic devices.<sup>2,8</sup> Thus, phase-modulation techniques are preferred for designing robust and reliable optical methods.<sup>1,2,4,8,9</sup>

To date, most measurement schemes based on phase-modulation techniques make use of sinusoidally modulated

excitation sources, and phase detection is performed at a single frequency with commercial lock-in amplifiers,<sup>9–12</sup> or either simple analog<sup>13,14</sup> or digital<sup>2,15,16</sup> implementations. However, the generation of a sinusoidal signal is not trivial, and therefore small-size, simple, low-cost, and low-power instruments cannot be easily developed for this purpose.<sup>17</sup> In addition, to avoid alteration of the signal waveform, continuous operation of the illumination source is required; it implies adding a direct current (dc) offset to the alternating current (ac) signal, and therefore it reduces the useful life of the sensor due to photodegradation processes.<sup>9,18,19</sup> Furthermore, the nonlinearities of several devices, such as LEDs, analog filters, amplifiers,

Received: September 26, 2013

Accepted: May 8, 2014

Published: May 8, 2014



photodetectors, etc., may produce a significant distortion in the sinusoidal waveform, resulting in undesirable measurement errors.<sup>17</sup>

To solve these problems, several authors have proposed the use of train of delta functions or square-wave excitations.<sup>4,5,20,21</sup> They offer a series of advantages with respect to sinusoidal excitation, such as (1) “on–off” operation of the light source that reduces the problems of nonlinear distortion of the signal waveform caused by nonlinear behavior of the electronic components; (2) simpler and lower-cost circuitry (i.e., quartz crystal oscillators, simple logic gates, transistors or micro-controllers); (3) higher power of signaling [i.e., better signal-to-noise ratio (SNR) for the modulated signal]; and (4) lower power consumption of the excitation light source,<sup>22</sup> ideal for implementation in battery-powered portable devices. In most of these schemes, the sensing phases are excited by use of light-emitting diode (LED) sources that are modulated with square-wave signals with a 50% duty cycle at a single frequency. Usually, only the information on lifetime estimated from phase shift or modulation factor of the fundamental harmonic is used.<sup>6,23</sup> However, another interesting feature of the square signals (in the frequency domain) is their multifrequency nature.<sup>24</sup> It supplies several advantages with respect to measurements at a single frequency,<sup>2,5</sup> although it has not been sufficiently exploited so far.

As the duty cycle in a rectangular signal decreases, the relative power of the high-order harmonics increases.<sup>24</sup> Therefore, a higher number of harmonics is available for multifrequency detection, avoiding the need to prepare complicated multifrequency excitation signals<sup>2</sup> or hard-implementation gated detection schemes.<sup>5</sup> In this paper we study the use of short duty cycle rectangular signals in phase-modulation-based luminescence spectroscopy. It provides simultaneous measurements of modulation factor and phase shift at several frequencies, leading to a more complete and reliable characterization of the luminescent system. Additionally, the apparent luminescence lifetimes (estimated from the modulation factor or the phase shift at different harmonics) provide a new strategy to obtain a more accurate determination of the analyte concentration. In order to improve the accuracy, we propose a method, formulated in a statistical framework, for combining the information provided by apparent luminescence lifetimes estimated from both modulation and phase shift at different harmonics. To the best of our knowledge, this is the first time that a multifrequency phase-modulation method with combination of information from more than one harmonic has been used in luminescence spectroscopy.

To develop the experimental work, an oxygen sensor has been selected as a well-known example of real applicability of the proposed method. In addition, a fiber optical sensor has been selected in order to have a relatively weak luminescence and low signal-to-noise ratio because it helps to observe the change in accuracy of the analyte determination.

## ■ THEORY: MULTIFREQUENCY LUMINESCENCE RESPONSE WITH RECTANGULAR-WAVE SIGNALS

### Measuring Modulation Factor and Phase Shift.

Conventionally, phase-modulation measurements estimate the luminescence response by use of a sinusoidally modulated excitation source. The phase shift and modulation factor are estimated by processing both excitation and emission signals at the modulation frequency. The use of short duty-cycle rectangular signals for excitation provides several harmonics

with enough amplitude for allowing the simultaneous measurement of phase shift and modulation factor at several frequencies. Since a conventional lock-in amplifier (LIA) allows the estimation of these parameters only at one frequency, a multifrequency scheme based on LIA would require a bank of LIAs (one for each harmonic to be used), including an appropriate band-pass filter at the input of each LIA. For multifrequency analysis of the response, we propose an analog-to-digital conversion and subsequent processing of the recorded digital signal, which can easily be implemented via software in a conventional computer or a microcontroller.

Analysis of the digitized signals [i.e., excitation,  $s_{\text{exc}}(t)$ , and emission,  $s_{\text{em}}(t)$ , signals] is performed in the frequency domain by applying the multifrequency in-phase/quadrature (I/Q) method.<sup>2</sup> At each harmonic  $f_i$ , the in-phase,  $I_e(f_i)$ , and quadrature,  $Q_e(f_i)$ , amplitudes are calculated from the digitized signal  $s_e(t)$  as

$$I_e(f_i) = \frac{1}{K} \sum_{t=0}^{T-1} s_e(t) \cos(2\pi f_i t / f_s) \quad (1)$$

$$Q_e(f_i) = \frac{1}{K} \sum_{t=0}^{T-1} s_e(t) \sin(2\pi f_i t / f_s) \quad (2)$$

where the subindex *e* stands for excitation (exc) or emission (em) signals, *i* is the index of the harmonic, *K* is a normalization constant, *t* is the index of the samples, *T* is the number of samples, and  $f_s$  is the sampling frequency.

From the in-phase and quadrature amplitudes, the amplitude and phase of the excitation and emission signals can be easily evaluated at each harmonic  $f_i$  as

$$A_e(f_i) = \sqrt{[I_e(f_i)]^2 + [Q_e(f_i)]^2} \quad (3)$$

$$\varphi_e(f_i) = -\arctan [Q_e(f_i)/I_e(f_i)] \quad (4)$$

and finally, taking into account the amplitude and phase of both signals, the modulation factor and phase shift are estimated at each harmonic as

$$m(f_i) = A_{\text{em}}(f_i)/A_{\text{exc}}(f_i) \quad (5)$$

$$\varphi(f_i) = \varphi_{\text{em}}(f_i) - \varphi_{\text{exc}}(f_i) \quad (6)$$

Although modulation factor has been defined in some works<sup>1</sup> as  $[A_{\text{em}}(f_i)/A_{\text{exc}}(f_i)]/[A_{\text{em}}(\text{dc})/A_{\text{exc}}(\text{dc})]$  (which requires estimation of the excitation and emission amplitudes at null frequency, that is, the dc component), we have used the definition in eq 5 because it only involves the amplitude at frequency  $f_i$ . This is an important practical advantage since the dc components are usually affected by offsets. One can note that, even though  $A_e(f_i)$  and  $\varphi_e(f_i)$  are biased depending on the normalization constant *K* and the time reference,  $m(f_i)$  and  $\varphi(f_i)$  remain invariant to them.

**Modeling Frequency Response of the Luminescent System.** From the modulation factor and phase shift, the complex frequency response can simultaneously be measured at different harmonics:

$$H(f_i) = m(f_i)e^{j\varphi(f_i)} \quad (7)$$

where *j* represents the imaginary unit. This way, from a set of multifrequency measurements, characterization of the luminescent system is possible. On the other hand, the complex

frequency response for a multiexponential luminescent system (also called multisite luminescent system) where luminescent changes are due to quenching is<sup>1</sup>

$$H(C, f) = \sum_j M_{0j} \frac{\tau_j(C)}{\tau_{0j}} \frac{1}{1 + j2\pi f \tau_j(C)} \quad (8)$$

where subindex  $j$  stands for each monoexponential process contributing to the global luminescent response,  $M_{0j}$  and  $\tau_{0j}$  are respectively the modulation factor at low frequency and null concentration and the lifetime at null concentration for process  $j$ , and  $\tau_j(C)$  is the lifetime associated with process  $j$ , described by a Stern–Volmer equation:

$$\tau_j(C) = \tau_{0j} \frac{1}{1 + k_j C} \quad (9)$$

where  $k_j$  is the Stern–Volmer constant for process  $j$  and  $C$  is the quencher concentration. By use of this equation, the frequency response of a multiexponential luminescent system can be rewritten as

$$H(C, f) = \sum_j \frac{M_{0j}}{1 + k_j C + j2\pi f \tau_{0j}} \quad (10)$$

Therefore, from a set of multifrequency measurements acquired at different quencher concentrations, a model (mono- or multiexponential) describing the luminescent response at different frequencies and concentrations can be estimated by finding the model parameters (i.e.,  $M_{0j}$ ,  $\tau_{0j}$  and  $k_j$ ) and minimizing the error between the measured frequency response (obtained from measured modulation factor and phase shift by use of eq 7) and the modeled frequency response in eq 10 (see Supporting Information section A for details).

**Estimation of Apparent Lifetime.** For a monoexponential system, the phase-shift-based lifetime  $\tau_\varphi(f_i)$  can be derived from the phase shift estimated at each harmonic as<sup>1</sup>

$$\tau_\varphi(f_i) = \frac{\tan[-\varphi(f_i)]}{2\pi f_i} \quad (11)$$

On the other hand, bearing in mind the relationship between lifetime  $\tau$  and modulation factor  $m(f)$  at frequency  $f$  for a monoexponential system:<sup>25</sup>

$$m(f) = M_0 \frac{\tau}{\tau_0} \frac{1}{\sqrt{1 + (2\pi f \tau)^2}} \quad (12)$$

(where  $\tau_0$  is the lifetime at null concentration of the quencher and  $M_0$  is the modulation factor at low frequency and null concentration), a modulation-factor-based lifetime ( $\tau_m$ ) can be estimated at each harmonic as (see Supporting Information section B for further details):

$$\tau_m(f_i) = \tau_0 \frac{m(f_i)/m_0(f_i)}{\sqrt{1 + (2\pi f_i \tau_0)^2 \{1 - [m(f_i)/m_0(f_i)]^2\}}} \quad (13)$$

where  $m_0(f_i)$  is the modulation factor at null concentration and frequency  $f_i$ . Estimation of  $\tau_m(f_i)$  requires measurement of the modulation factor  $m(f_i)$  and two additional parameters,  $m_0(f_i)$  and  $\tau_0$ . These last two parameters can be estimated from calibration measurements at null concentration and eq 11.

If the system is accurately described by a monoexponential model, estimations of  $\tau_\varphi(f_i)$  and  $\tau_m(f_i)$  obtained at different frequencies would be the same. However, the one-site

monoexponential model is usually insufficient for describing most real luminescent systems and the lifetimes estimated at different frequencies are not expected to provide the same value. In such situation, these estimations are preferably called apparent lifetimes.<sup>1</sup>

The proposed multifrequency method provides, therefore, the modulation factor and the phase shift at several modulation frequencies simultaneously. These parameters can be applied for obtaining a complete description of the luminescent system frequency response, for different modulation frequencies and quencher concentrations, by fitting appropriate mono- or multiexponential models. These parameters also can be applied for estimating the apparent lifetimes at different frequencies, either from the modulation factor,  $\tau_m(f_i)$ , or from the phase shift,  $\tau_\varphi(f_i)$ .

#### Determination of Quencher Concentration and Combination of Concentration Measurements.

Determination of quencher concentration can be performed by use of calibration curves appropriately fitted from calibration data. Calibration and determination of the quencher concentration could be performed by use of the model describing the global frequency response or by use of specific calibration curves for each lifetime parameter [i.e., for  $\tau_m(f_i)$  and  $\tau_\varphi(f_i)$  at each specific harmonic]. A model describing the global frequency response at different frequencies and quencher concentrations is useful, since it allows prediction of the behavior of the luminescent system in a wide variety of conditions. However, accurate determination of the quencher concentration requires accurate modeling of the luminescent system response as a function of the concentration. Obtaining a very accurate calibration with a global modeling of the response is difficult, because usually real luminescent systems approximately behave as low-order exponential systems, but there are deviations in the frequency response (model residual) that cannot be modeled with the multiexponential model. For this reason, determining the quencher concentration from the apparent lifetimes (by use of an independent calibration curve for each lifetime parameter) is preferable. Since the proposed method simultaneously provides  $\tau_m(f_i)$  and  $\tau_\varphi(f_i)$  at several harmonics, different calibration curves can be fitted independently for each parameter. Similarly, from a single signal recording [ $s_{em}(t)$  and  $s_{exc}(t)$ ], different independent determinations of the quencher concentration can be estimated. From  $N$  unbiased and statistically independent determinations of the quencher concentration  $\tilde{C}(x_n)$  (each one based on an estimated parameter  $x_n$  with  $n = 1, 2, \dots, N$ ), a more accurate estimation  $\hat{C}$  can be obtained as the expected value of  $C$  from the joint probability distribution (see Supporting Information section C for details of the mathematical derivation):

$$\hat{C} = \frac{\sum_{n=1}^N \tilde{C}(x_n) \prod_{k \neq n} \sigma_k^2}{\sum_{n=1}^N \prod_{k \neq n} \sigma_k^2} \quad (14)$$

where  $\sigma_n$  is the standard error associated with the  $n$ th measurement  $\tilde{C}(x_n)$ , that could also be noted as  $SE[\tilde{C}(x_n)]$ . Since the quencher concentration  $\tilde{C}(x_n)$  is estimated from the parameter  $x_n$  (where  $x_n$  is a phase- or modulation-based apparent lifetime) by using the corresponding calibration curve, the standard error  $SE[\tilde{C}(x_n)]$  can be estimated according to error propagation theory as



$$\sigma_n = \text{SE}[\tilde{C}(x_n)] = \left| \frac{\partial \tilde{C}(x_n)}{\partial x_n} \right| \text{SE}(x_n) \quad (15)$$

where  $\tilde{C}(x_n)$  is the calibration function describing the quencher concentration as a function of the parameter  $x_n$ , and the standard error  $\text{SE}(x_n)$  should be obtained from several measurements acquired in the operation conditions. However, estimation of the combined concentration  $\hat{C}$  does not require the standard errors, but the standard errors relative to one of them (i.e., if all the standard errors are multiplied by a constant,  $\hat{C}$  remains invariant). Therefore, if we accept that under the measurement conditions (due to the unknown noise conditions) the standard errors  $\text{SE}(x_n)$  (and  $\sigma_n$ ) are scaled with a constant that depends only on the signal-to-noise ratio (SNR), then in eq 14  $\hat{C}$  remains invariant if we apply the standard errors estimated at a reference SNR condition to the measurements acquired at a different SNR condition. Therefore, the standard errors for eq 14 could be estimated from the calibration data.

This way, the proposed method can be applied to combine the information obtained from  $\tau_m(f_i)$  and  $\tau_\varphi(f_i)$  at different harmonics when the system is excited with a short duty cycle rectangular-wave signal.

## ■ EXPERIMENTAL SECTION

**Chemicals and Reagents.** Platinum(II) *meso*-tetra-(pentafluorophenyl)porphine (PtTFPP) was purchased from Frontier Scientific Inc. (Logan, UT) and was used as oxygen-sensitive dye. Polystyrene (PS; 280 000 g·mol<sup>-1</sup>), which was used as solid support, and chloroform (used as solvent) were purchased from Sigma–Aldrich. All chemicals and reagents were of analytical grade and were used as received without further purification.

**Preparation of Sensing Fiber.** A fiber optical sensor has been selected in order to have a relatively weak luminescence and low SNR. It helps to observe the change in accuracy in the analyte determination. A multimode plastic-clad silica optical fiber (OFS, Norcross, GA; core/cladding diameters 200/230  $\mu\text{m}$ , attenuation of 4.28 dB/km at 650 nm, 1.5 m length, and SMA-905 connector at one end) was cut perpendicularly with a Fujikura CT-20-12 precision fiber cleaver, and a Leica DM2500 microscope (Leica Microsystems, Wetzlar, Germany) was used to visualize images of the optical fiber (see Supporting Information, Figure SI-2). A portion (2 cm) of the optical fiber plastic cladding was removed by means of a flame burner. Finally, the optical fiber was cleaned with absolute ethanol to eliminate dirt and impurities.

The membrane cocktail was prepared by mixing thoroughly 396 mg of PS, 6 mg of PtTFPP, and 4.0 mL of chloroform in a glass vial (dye concentration 1.5 mg·mL<sup>-1</sup>). The mixture was continuously stirred until complete dissolution and then coated on the clean, cladding-free optical fiber by dip coating on a Nadetech ND-R rotatory dip coater (Nadetech Innovations, Pamplona, Spain)<sup>26–28</sup> with a dipping speed of 11 mm/s, dipping time of 1 s, and raising speed of 11 mm/s. Finally, the sensing film was dried in an oven at 40 °C for 10 min.<sup>26</sup> Figure SI-3 in Supporting Information shows some SEM images of the coated optical fiber obtained with a Carl Zeiss FE-SEM Ultra Plus microscope (Carl Zeiss Microscopy). The estimated thickness of the coated layer was 1028  $\pm$  123 nm (95% confidence interval).

**Measurement System.** Figure SI-1 in Supporting Information displays a schematic diagram of the experimental setup used in this work. It is based on simple modifications of the experimental setup described by our research group for implementing the I/Q method.<sup>2</sup>

To mix nitrogen and oxygen (both of 99.999% purity, obtained from Air Liquide España) two mass-flow controllers (MFCs) (EL-FLOW Select F-201CV, Bronkhorst High-Tech, Ruurlo, The Netherlands) connected to a flow-bus interface (Bronkhorst High-Tech) via a RS-232 serial port were used. The MFCs were connected, via copper and stainless steel tubing, to the flow-through cell, which was designed in our laboratory and uses a standard glass tube (230 mm in length) to hold the optical fiber probe.

The optical fiber probe was excited with an ultraviolet LED (Ocean Optics, LS-450 LED-395,  $\lambda_{\text{max}} = 391$  nm, angle of illumination 15°, LED diameter 5 mm, luminous power 25  $\mu\text{W}$ ) filtered through an optical band-pass filter (OF-1; Thorlabs GmbH, MF390-18,  $\lambda_{\text{central}} = 390$  nm). This LED was modulated by use of two different analogue current signals: (1) a sine-wave signal of 5145 Hz and (2) a rectangular-wave signal (with 10% duty cycle) of 1715 Hz. The excitation signal was numerically generated with a computer and was provided by the analog output channel on an AD/DA board (NI PCIe-6363/BNC-2120, National Instruments) at a sampling rate of 500 kS/s. This excitation signal was applied to the LED driving circuit in order to modulate the current in the LED. The voltage in a resistor in series with the LED was used as reference excitation signal,  $S_{\text{exc}}(t)$  (see Figures SI-4 and SI-5 in Supporting Information for further details). The emission signal was transduced with a photomultiplier tube (PMT) with a bandwidth dc–1 MHz (H10723-20, Hamamatsu Photonics, Japan) equipped with an appropriate optical band-pass filter, and the PMT output was amplified and filtered with appropriate analog electronics. Both the excitation signal (the reference) and the emission signal from the sensing film were simultaneously digitized via a digital oscilloscope WaveRunner 604Zi (LeCroy) at 500 kS/s using signals of 200 ms in duration (i.e., a 100 kS data buffer). The bandwidth of the electronic devices and the sampling rates are large enough for the frequency of the harmonics involved in these experiments and they are also appropriate for the typical lifetimes of the used indicator (that is, for lifetimes in the range of tens of microseconds). The proposed method could also be applied to indicators with shorter lifetimes by using a higher fundamental frequency in the rectangular-wave signals, and hardware components with appropriate bandwidth. In the experimental setup, the element conditioning the frequency range is the PMT, which has a bandwidth of 1 MHz. This limits the minimum lifetime that can be measured to around 0.1  $\mu\text{s}$  (for measuring luminophores with a shorter lifetime, a faster PMT should be used, and the preamplifier and analog filters should be redesigned).

All measurements were performed at room temperature (21 °C). The temperature was continuously monitored by a commercial temperature sensor (MicroLite, Fourtec-Fourier Technologies).

**Implementation of Rectangular-Wave Modulated Excitation in Phase-Modulation Methods.** In order to demonstrate the ability of the proposed multifrequency phase-modulation method based on a rectangular-wave modulated excitation source with a short (10%) duty cycle, it was compared with a conventional phase-modulation method based

on a sinusoidally modulated excitation signal using the same luminescence system (see Figure 1). To ensure a fair

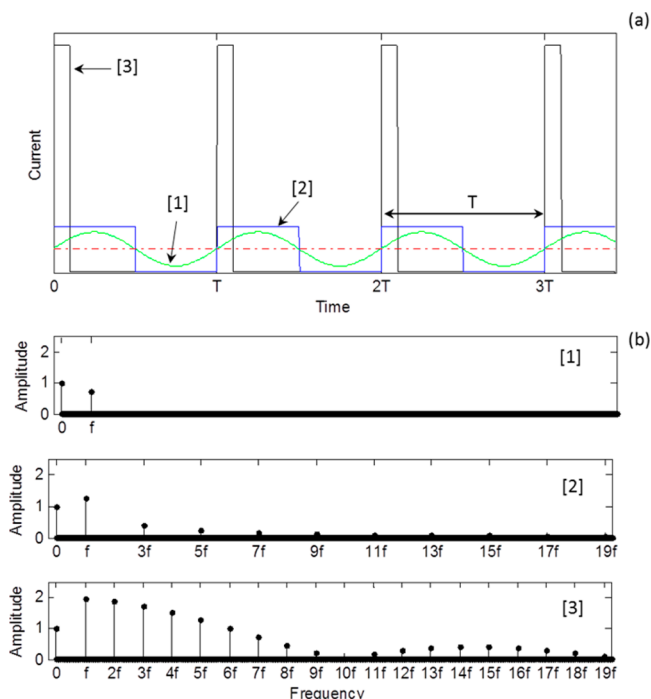


**Figure 1.** (a) Waveform and (b) amplitude spectrum of [1] sinusoidal wave, [2] square wave with 50% duty cycle, and [3] rectangular wave with 10% duty cycle with the same average current level (dot-dashed line).

comparison, the waveforms must have equal total excitation energy over the time course of the experiment. Thus, if it is

assumed that these waveforms were used to modulate the electrical current of a LED excitation source, all of them had the same average current level (see horizontal dot-dashed line in Figure 1a or amplitude of the dc component (i.e., 0 Hz) in Figure 1b) to ensure the same average electrical power dissipated by the LED (directly related to its average optical output power).<sup>29</sup>

As can be seen in Figure 1b [2], a 50% duty cycle square-wave excitation has a very rapid falloff in amplitude of the higher harmonics and only the odd harmonics have non-null amplitude. Therefore, the standard method with square-wave excitation is limited to at most a few harmonics.<sup>5</sup> This drawback can be solved by use of a short (10%) duty cycle rectangular-wave excitation, which has a slow falloff in the amplitude of both even and odd harmonics (see Figure 1b [3]). Thus, rectangular-wave signals are ideal for multifrequency analysis, since simultaneous measurements of the luminescence are possible at a number of frequencies by use of the calculated phases and/or amplitudes for several harmonics of the excitation and emission waveforms.

Two types of excitation signals have been used in this study: (1) a conventional sinusoidal signal (frequency 5145 Hz), used as reference, and (2) the proposed 10% duty cycle rectangular-wave signal (fundamental frequency 1715 Hz). In the case of the sinusoidal signal, modulation factor, phase shift, and the corresponding modulation- and phase-based apparent lifetimes ( $\tau_m$  and  $\tau_\phi$ ) at 5145 Hz have been estimated by the I/Q method.<sup>2</sup> In the case of the rectangular wave, these parameters have been estimated for the five first harmonics (i.e., 1715, 3430, 5145, 6860, and 8575 Hz) with the multifrequency I/Q method.<sup>2</sup> Figure SI-5 in Supporting Information shows some examples of signals and the corresponding spectra.

Implementation of the proposed method requires, on one hand, a rectangular signal (instead of a sinusoidal one) to be

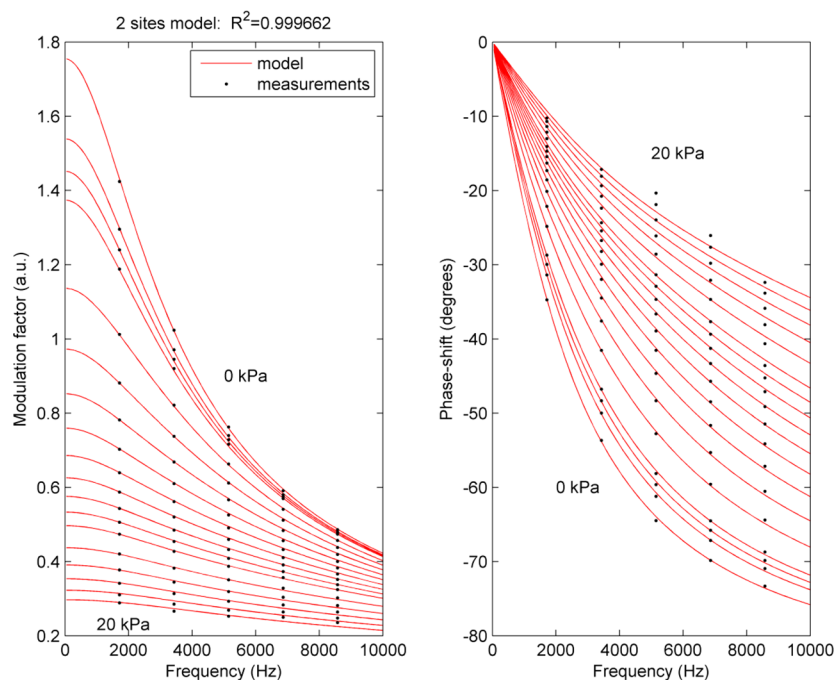


**Figure 2.** Frequency response of the two-sites model estimated for fitting the measured modulation factor and phase shift. Left panel, modulation factor; right panel, phase shift. Frequency response of the model is shown with solid lines; experimental measurements are shown with points. Measurements were recorded at concentrations 0, 0.5, 0.75, 1, 2, 3, 4, 5, 6, 7, 8, 9, 10, 12, 14, 16, 18, and 20 kPa O<sub>2</sub>. Model parameters:  $M_{01} = 1.4413$ ;  $k_1 = 0.32278 \text{ kPa}^{-1}$ ;  $\tau_{01} = 60.31 \text{ } \mu\text{s}$ ;  $M_{02} = 0.3134$ ;  $k_2 = 0.10108 \text{ kPa}^{-1}$ ;  $\tau_{02} = 89.60 \text{ } \mu\text{s}$ .

used as excitation signal and, on the second hand, the multifrequency I/Q algorithm to process the recorded digital signal in order to obtain the phase shift and modulation factor at each harmonic. In our setup, the change from a sine-wave signal to a rectangular-wave signal is trivial, since an AD/DA board was used in both cases. In general, the use of an on–off rectangular signal simplifies the electronics with respect to the use of sinusoidal signals (the electronic design of a sinusoidal oscillator with low harmonic distortion is significantly more complicated and expensive than a rectangular-wave oscillator). On the other hand, the multifrequency I/Q method increases the sophistication of the algorithm, but it just involves digital signal processing (that is easily implemented in software and therefore would not limit the portability of a measuring system based on the proposed method). Acquisition of digital signals was performed with a digital oscilloscope (which limits the portability), but AD conversion can be easily implemented with an AD/DA board connected to a laptop in order to increase portability.

## ■ RESULTS AND DISCUSSION

**Characterization of Luminescent System.** Eighteen concentrations, ranging between 0 and 20 kPa O<sub>2</sub>, were analyzed by recording 200 ms signals for each concentration level and using both sinusoidal and rectangular-wave signals to excite the sensing film (625 excitation and emission signals were recorded at each condition). Phase shifts and modulation factors were calculated from eqs 6 and 5, respectively, at the modulation frequency in the case of sine wave and at the five first harmonics for the rectangular wave. Mean and standard deviation values for the phase shifts and modulation factors at different oxygen concentrations and frequencies (for both sine-wave and rectangular-wave signals) are shown in Supporting Information (see Tables SI-1 and SI-3 and Figure SI-6). The modulation factor decreases with both oxygen concentration and modulation frequency. The phase shift is in the range between  $-90^\circ$  and  $0^\circ$ , and its absolute value increases with modulation frequency and decreases with oxygen concentration. This is in accordance with the expected frequency response of a mono- or multiexponential system. A comparison of the modulation factor and phase-shift measurements for the modulation frequency of 5145 Hz using sinusoidal excitation signal and those for the third harmonic using the rectangular-wave signal (also 5145 Hz) reveals very similar values in both cases: phase shifts differ less than  $0.15^\circ$  and modulation factors differences are smaller than 1% (see Tables SI-1 and SI-3 in Supporting Information).

The experimental frequency response (eq 7) has been modeled as a monoexponential and as a biexponential system (eq 10). Figure 2 shows the modulation factor and phase-shift curves provided by the biexponential (two-sites) model at different concentrations and modulation frequencies. This figure also includes the experimental modulation factors and phase shifts. The monoexponential (one-site) model is represented in Figure SI-7 (Supporting Information). The monoexponential model shows a determination coefficient  $R^2 = 0.995\,437$  (i.e., the residual is 0.4563% of the variance in the experimental data). The high value of  $R^2$  reveals that the monoexponential model provides a reasonable approach to the global frequency response of the luminescent system at different oxygen concentrations. The determination coefficient significantly increases when the two-sites model is used to fit experimental data ( $R^2 = 0.999\,662$ , with a residual of 0.0338%

of the variance in the experimental data, that is, more than 10 times smaller than in the monoexponential model), and therefore, this model significantly improves the global description of the luminescent system. A three-sites model provides a determination coefficient  $R^2 = 0.999\,695$ , that is, with no significant improvement in description of the luminescent system with respect to the two-sites model. The two sites model is appropriate for a global description of the two sites model, particularly for lower concentrations of oxygen (i.e., when modulation factors are greater). The residual error is more evident for the phase shift, particularly in those situations with lower modulation factors due to the criterion used for model fitting (minimum mean square error).

Fitting a multiexponential model to some experimental data implies the estimation of three parameters for each exponential process (i.e.,  $M_{0j}$ ,  $\tau_{0j}$ , and  $k_j$ ). Since experimental data are always affected by some level of noise and the luminescent system could also include some additional processes (not modeled by multiexponential equations), the availability of enough experimental data is critical for appropriate model fitting (the number of conditions involved in the fitting should be significantly greater than the number of parameters to be estimated). In this sense, the proposed multifrequency method is valuable since it provides experimental data simultaneously at several harmonics. The validation of a model describing some experimental data is usually performed by comparing the residual obtained with some calibration data and the residual obtained with test data, that is, data different than those used for calibration.<sup>30</sup>

In order to analyze the advantages of using several harmonics for characterization of the luminescent system, a two-sites model has been estimated using only the modulation factors and phase shifts from the third harmonic (this situation would be equivalent to the use of the sinusoidal signal), and another two-sites model has been estimated from the modulation factors and phase shifts from the second, third, and fourth harmonics. Both models have been evaluated by comparing the predicted frequency response with the measured frequency response at first and fifth harmonics. The results are shown in Supporting Information (see Figure SI-8). When only the third harmonic is used for model estimation, the determination coefficient increases to  $R^2 = 0.999\,905$  for the calibration data (third harmonic), but it decreases to  $R^2 = 0.989\,650$  for the test data (first and fifth harmonics). On the other hand, the two-sites model estimation based on second, third, and fourth harmonics provides a determination coefficient  $R^2 = 0.999\,455$  for the calibration data that remains stable for the test data ( $R^2 = 0.999\,543$ ). This illustrates that a model estimation based on just one harmonic is insufficient, while the use of information from several harmonics (based on the proposed multifrequency I/Q method) allows the estimation of a model that improves the global frequency response description of the luminescent system.

This improved description of the global frequency response at different concentrations can also be observed when the two-sites model is calibrated with some oxygen concentrations and evaluated with others. When the model is calibrated with measurements at concentrations 2, 3, 4, 5, 6, 7, 8, 9, 10, and 12 kPa and evaluated with measurements at 0, 0.5, 0.75, 1, 14, 16, 18, and 20 kPa, the determination coefficients are  $R^2_{\text{cal}} = 0.999\,755$  and  $R^2_{\text{test}} = 0.999\,538$  for calibration and test data, respectively. Moreover, when the two-sites model is calibrated with measurements just at two concentrations (1 and 6 kPa)



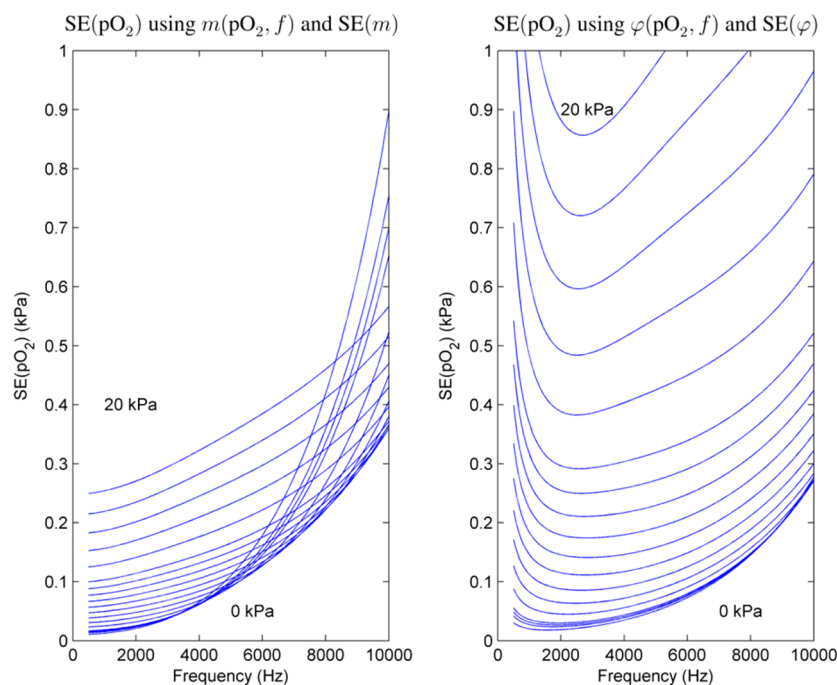


**Figure 3.** Standard error of oxygen determination,  $SE(pO_2)$ , as a function of modulation frequency when the determination is based on modulation factor (left panel) or phase shift (right panel). Curves correspond to the concentrations 0, 0.5, 0.75, 1, 2, 3, 4, 5, 6, 7, 8, 9, 10, 12, 14, 16, 18, and 20 kPa  $O_2$ . The estimation of  $SE(pO_2)$  includes the standard error associated with the measured parameters.

and evaluated with all the other concentrations, the observed determination coefficients are  $R^2_{cal} = 0.999\,911$  and  $R^2_{cal} = 0.999\,233$ , respectively (see Figure SI-9 in Supporting Information).

When the accurate description of the luminescent system (at different quencher concentrations and frequencies) provided by the two-sites model calibrated with measurements at several harmonics is taken into account, it can be concluded that use of the proposed multifrequency method provides a more detailed description of the system than use of sine-wave signals, since it simultaneously provides information at different frequencies from just one measurement. This advantage is very useful for complete description and fast characterization of the luminescent system.

**Analysis of Optimal Modulation Frequency.** Characterization of the global luminescent response is also useful for analysis of optimal modulation frequency. This can be defined as the frequency for which the standard error of the determined quencher concentration  $SE(C)$  is minimal. This standard error can be estimated from the frequency response of the luminescent system and the standard error of modulation factor or phase-shift measurements,<sup>25</sup> by applying error propagation theory:

$$SE(C_m) = \left| \frac{\partial C}{\partial m} \right| SE(m) = \frac{1}{\left| \frac{\partial m(C, f)}{\partial C} \right|} SE(m) \quad (16)$$

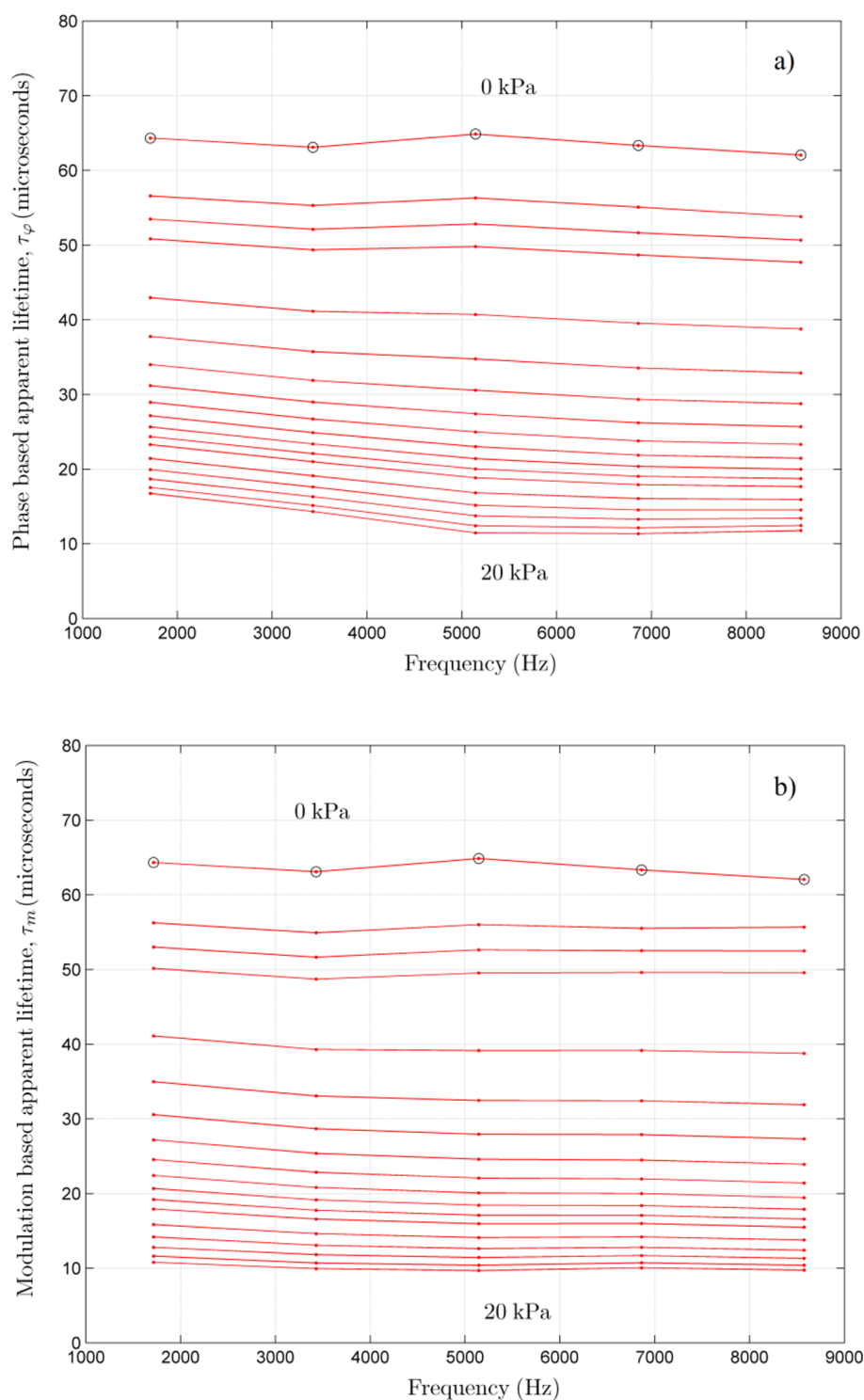
$$SE(C_\varphi) = \left| \frac{\partial C}{\partial \varphi} \right| SE(\varphi) = \frac{1}{\left| \frac{\partial \varphi(C, f)}{\partial C} \right|} SE(\varphi) \quad (17)$$

Figure 3 shows the expected standard error in  $pO_2$  determination for different oxygen concentrations as a function of frequency when the determination is based on modulation factor (left panel) or phase shift (right panel). In order to

obtain these plots, the global two-sites model in Figure 2 was used for obtaining the partial derivatives, and models describing the observed standard errors  $SE(m)$  and  $SE(\varphi)$  at different concentrations and modulation frequencies have been fitted from the experimental data (see Figure SI-10 in Supporting Information for further details). Figure 3 shows that oxygen determination based on modulation factor is optimal for very low frequencies (ideally at null frequency, even though estimation of the modulation factor at dc is not recommendable due to instrumental offsets). On the other hand, oxygen determination based on phase shift presents a well-defined optimal frequency, which slightly increases with oxygen concentration. This behavior would be significantly different if standard errors  $SE(m)$  and  $SE(\varphi)$  were ignored (i.e., if only the partial derivatives are considered in eqs 16 and 17), as described previously by Ogurtsov and Papkovski.<sup>25</sup> Figure SI-11 (Supporting Information) shows the  $SE(pO_{2m})$  and  $SE(pO_{2\varphi})$  computed without  $SE(m)$  and  $SE(\varphi)$ . Under this last approach, the oxygen determination based on phase shift presents an optimal frequency that strongly increases with concentration. The differences between the two approaches for computing optimal modulation frequency are due to reduction of the luminescent response with frequency and quencher concentration and the subsequent reduction of the signal-to-noise ratio: an appropriate analysis of optimal modulation frequency should consider not only the sensitivity of the luminescent system but also the noise affecting the measurements.

**Estimation of Apparent Lifetimes and Calibration.** The phase shift-based apparent lifetime ( $\tau_\varphi$ ) and the modulation-based apparent lifetime ( $\tau_m$ ) were estimated by use of eqs 11 and 13 from the corresponding phase shifts and modulation factors [the parameters  $m_0(f_i)$  and  $\tau_0$  were estimated from calibration data at null concentration]. The estimated apparent lifetimes for different concentrations and





**Figure 4.** Effect of modulation frequency on apparent luminescent lifetimes estimated from (a) phase shift and (b) modulation factor at 0, 0.5, 0.75, 1, 2, 3, 4, 5, 6, 7, 8, 9, 10, 12, 14, 16, 18, and 20 kPa  $\text{O}_2$ .

modulation frequencies (using both sine-wave and rectangular-wave signals) and the corresponding standard deviations can be seen in Supporting Information (see Tables SI-2 and SI-4; Figure SI-13 shows the standard deviation).

Figure 4 shows the phase shift-based apparent lifetime ( $\tau_\varphi$ ) and the modulation-based apparent lifetime ( $\tau_m$ ) as a function of modulation frequency, estimated for different oxygen concentrations when the rectangular-wave signal is used. The apparent lifetime decreases from 65 to 10  $\mu\text{s}$  when the oxygen

concentration increases from 0 to 20 kPa  $\text{pO}_2$ . If a monoexponential luminescence model is assumed, for a given oxygen concentration, the phase shift-based apparent lifetime should be the same as that obtained from modulation factor, and also when they are estimated for different harmonics. However, significant differences are observed. In general, an increase of the apparent lifetime is observed for lower frequencies; this increase is more important when the lifetime is estimated from the phase shift. Finally, similar values of  $\tau_\varphi$

and  $\tau_m$  can be observed for lower concentrations (as expected from eq 13), but  $\tau_\phi$  is significantly higher than  $\tau_m$  for high concentrations. Therefore, this multifrequency analysis of the apparent lifetimes confirms that the monoexponential luminescence model is insufficient for describing this sensing phase.

With the residual in the global two-sites model describing the response of the luminescent system at all frequencies and concentrations taken into account, calibration oriented to the determination of oxygen concentration was performed independently for each estimation of the apparent lifetime. The estimated  $\tau_\phi$  and  $\tau_m$  obtained at different frequencies (see Supporting Information, Table SI-2 for sine-wave signals and Table SI-4 for rectangular-wave signals) were used for calibrating. Calibration curves were obtained by fitting experimental data by use of the Demas two-site model.<sup>31</sup> The resulting calibration curves and model parameters are shown for sine-wave and rectangular-wave signals (see Supporting Information, Figure SI-14 and Tables SI-5 and SI-6). These calibration curves were used for the determination of the oxygen concentration.

When the apparent lifetimes are estimated by use of rectangular-wave signals, smaller standard deviations are observed even for higher-order harmonics (see Supporting Information, Tables SI-2 and SI-4 and Figure SI-13). This is due to the higher amplitude of the harmonics (compared to the amplitude of the frequency component for the sine-wave signal) at equal illumination conditions and suggests that use of the proposed rectangular-wave signals would provide a more accurate determination of oxygen concentration.

After calibration of the system, the analyte concentration can be determined from the recorded signal when the system is excited with a sinusoidal signal or a rectangular-wave signal. In the case of the sinusoidal signal,  $\tau_\phi$  and  $\tau_m$  are obtained and two estimations of the analyte concentration [ $p\tilde{O}_2(\tau_\phi)$  and  $p\tilde{O}_2(\tau_m)$ ] are available (one from  $\tau_\phi$  and one from  $\tau_m$ ) by application of the corresponding calibration curve. In the case of the rectangular-wave signal, five harmonics were analyzed, and 10 parameters are available [ $\tau_\phi(f_i)$  and  $\tau_m(f_i)$  for  $i = 1-5$ ] from each recorded signal. Therefore, by applying the corresponding calibration curve, 10 independent estimations of the analyte concentration are available [ $p\tilde{O}_2[\tau_\phi(f_i)]$  and  $p\tilde{O}_2[\tau_m(f_i)]$  for  $i = 1-5$ ].

Therefore, the analyte concentration could be determined by using one of these parameters alone (for each parameter, one concentration may be determined), or the estimations from different parameters could be combined in order to increase the accuracy in determination of the concentration. In the case of sinusoidal signal, only two  $p\tilde{O}_2$  measurements are available while the rectangular-wave signal allows combination of the information from several harmonics (in our case the combination of up to 10 parameters).

**Evaluation of Accuracy of the Proposed Method.** The simple algorithm described in eq 14 can be applied to combine the information obtained from  $\tau_\phi(f_i)$  and  $\tau_m(f_i)$  when the system is excited with a sinusoidal signal or a rectangular-wave signal. Moreover, the algorithm can be applied to combine multifrequency information provided by different harmonics in the case of the rectangular-wave signal.

The proposed method has been evaluated for both sinusoidal and rectangular-wave excitation signals. For 17 values of oxygen concentration (ranging between 0.5 and 20 kPa), 625 measurements (different than those used for calibrating) were recorded with each excitation signal (sine-wave and rectangular-

wave), using the same sensing film and exciting it with the same average luminous power. For each measurement, estimations of the analyte concentration  $p\tilde{O}_2$  have been obtained from  $\tau_\phi$  and  $\tau_m$ . Two estimations of concentration based on one parameter have been obtained in the case of sinusoidal excitation signals (one from  $\tau_\phi$  and the other from  $\tau_m$ ). In the case of rectangular-wave excitation signals, 10 estimations of concentration were obtained (from  $\tau_\phi$  and  $\tau_m$  for the five first harmonics). In addition to the concentration estimations based on one parameter, several combinations have been evaluated, including information from  $\tau_\phi$  and  $\tau_m$  or combining information from different harmonics in the case of rectangular-wave signals.

Evaluation of accuracy was based on the root-mean-square error (RMSE), with the measurements from the mass-flow controllers used as reference. Tables SI-7–SI-9 in Supporting Information show detailed experimental results for both excitation signals, including concentrations estimated from  $\tau_\phi$ ,  $\tau_m$ , and the combination of both, and also combining estimations from different harmonics (in the case of rectangular-wave signals). Table 1 and Figure 5 summarize these results.

They show that, for the same luminous power, the first harmonics from the rectangular-wave signal provides better accuracy than the sinusoidal signal at low and high concentration levels. This is because the power of these harmonics is higher than that for the fundamental frequency in the sinusoidal signal (and the SNR is consequently higher), as can be seen in Figure 1. Analogously, concentrations estimated from harmonics in the rectangular-wave signals are more accurate for the lower-order harmonics due to their higher power (and higher SNR).

Experimental results also show that the procedure proposed for combining information from several parameters for determining analyte concentration is very efficient. The combination of  $\tau_\phi$  and  $\tau_m$  provides better accuracy than each of them separately, in all cases. In addition, the proposed method provides an appropriate combination of the information obtained from different harmonics. As can be seen in Table 1, the inclusion of a new harmonic generally improves the accuracy in determination of the analyte concentration, and this is observed for estimations based on  $\tau_\phi$  (RMSE reduced from 0.1588 to 0.0781 at 6 kPa  $O_2$ ), those based on  $\tau_m$  (RMSE reduced from 0.0693 to 0.0546 at 6 kPa  $O_2$ ), or those based on a combination of both  $\tau_\phi$  and  $\tau_m$  (RMSE reduced from 0.0613 to 0.0474 at 6 kPa  $O_2$ ). In addition, the experimental results show that use of the proposed multifrequency phase-modulation method provides a more accurate determination, reducing RMSE from 0.1627 to 0.0128 kPa at 0.5 kPa  $O_2$  and from 0.9393 to 0.1532 kPa at 20 kPa  $O_2$  when it is compared with a conventional phase-modulation method based on a sinusoidally modulated excitation source (under equal luminous power conditions).

Comparison between the RMSE observed in determination of oxygen concentration from modulation factor or phase shift at just one harmonic (Table 1 and Table SI-8 in Supporting Information) and the expected standard error presented in Figure 3 shows a remarkable coincidence between both. This coincidence confirms the utility of the multifrequency phase-modulation method for accurately describing the global frequency response of the luminescent system and for analysis of the optimal modulation frequency.

Determinations of the concentration based on  $\tau_m$  are generally more accurate than those based on  $\tau_\phi$  in all the

**Table 1. Accuracy for Several Combinations with Conventional and Proposed Multifrequency Phase-Modulation Methods in Determination of pO<sub>2</sub> at Four Oxygen Concentration Levels**

parameter	frequency	RMSE (kPa)			
		0.5 kPa O <sub>2</sub>	2.0 kPa O <sub>2</sub>	6.0 kPa O <sub>2</sub>	20 kPa O <sub>2</sub>
Sine-Wave Excitation <sup>a</sup>					
$\tau_\phi$	$f_{\sin}$	0.1788	0.2476	0.5067	3.0893
$\tau_m$	$f_{\sin}$	0.3128	0.2710	0.3353	0.9947
$\tau_\phi, \tau_m$	$f_{\sin}$	0.1627	0.1948	0.2722	0.9393
Rectangular-Wave Excitation <sup>b</sup>					
$\tau_\phi$	$f_1$	0.0215	0.0404	0.1588	0.9792
$\tau_\phi$	$f_2$	0.0326	0.0537	0.1413	0.7907
$\tau_\phi$	$f_3$	0.0534	0.0776	0.1615	0.9760
$\tau_\phi$	$f_4$	0.0958	0.1375	0.2776	1.1020
$\tau_\phi$	$f_5$	0.1476	0.1763	0.2625	1.0456
$\tau_\phi$	$f_1, f_2$	0.0181	0.0320	0.1039	0.5892
$\tau_\phi$	$f_1, f_2, f_3$	0.0173	0.0298	0.0850	0.4804
$\tau_\phi$	$f_1, f_2, f_3, f_4$	0.0170	0.0296	0.0810	0.4451
$\tau_\phi$	$f_1, f_2, f_3, f_4, f_5$	0.0168	0.0296	0.0781	0.4051
$\tau_\phi$	$f_3, f_4, f_5$	0.0497	0.0650	0.1196	0.6100
$\tau_m$	$f_1$	0.0221	0.0325	0.0693	0.2445
$\tau_m$	$f_2$	0.0455	0.0501	0.0846	0.2872
$\tau_m$	$f_3$	0.1013	0.0906	0.1225	0.3796
$\tau_m$	$f_4$	0.2371	0.2229	0.2245	0.6403
$\tau_m$	$f_5$	0.3467	0.3091	0.2737	0.6508
$\tau_m$	$f_1, f_2$	0.0194	0.0285	0.0566	0.1840
$\tau_m$	$f_1, f_2, f_3$	0.0194	0.0278	0.0540	0.1701
$\tau_m$	$f_1, f_2, f_3, f_4$	0.0193	0.0276	0.0540	0.1659
$\tau_m$	$f_1, f_2, f_3, f_4, f_5$	0.0193	0.0274	0.0546	0.1626
$\tau_m$	$f_3, f_4, f_5$	0.0884	0.0830	0.1083	0.2853
$\tau_\phi, \tau_m$	$f_1$	0.0155	0.0251	0.0613	0.2369
$\tau_\phi, \tau_m$	$f_2$	0.0265	0.0376	0.0767	0.2671
$\tau_\phi, \tau_m$	$f_3$	0.0482	0.0591	0.1018	0.3689
$\tau_\phi, \tau_m$	$f_4$	0.0924	0.1250	0.1800	0.5403
$\tau_\phi, \tau_m$	$f_5$	0.1348	0.1543	0.1896	0.5771
$\tau_\phi, \tau_m$	$f_1, f_2$	0.0135	0.0214	0.0501	0.1746
$\tau_\phi, \tau_m$	$f_1, f_2, f_3$	0.0131	0.0204	0.0478	0.1620
$\tau_\phi, \tau_m$	$f_1, f_2, f_3, f_4$	0.0129	0.0205	0.0475	0.1573
$\tau_\phi, \tau_m$	$f_1, f_2, f_3, f_4, f_5$	0.0128	0.0204	0.0474	0.1532
$\tau_\phi, \tau_m$	$f_3, f_4, f_5$	0.0464	0.0529	0.0861	0.2747

<sup>a</sup> $f_{\sin} = 5145$  Hz. <sup>b</sup> $f_1 = 1715$  Hz,  $f_2 = 3430$  Hz,  $f_3 = 5145$  Hz,  $f_4 = 6860$  Hz, and  $f_5 = 8575$  Hz.

measurements (except for higher harmonics at low concentration). This is related to the typical standard error in the estimates of  $\tau_m$  or  $\tau_\phi$  (see Supporting Information, Tables SI-2 and SI-4 and Figure SI-13) and the associated standard error in concentration estimations due to error propagation. It was previously described in other works.<sup>2,9</sup> However, the measurements based on  $\tau_\phi$  are usually preferred since modulation factors are usually more biased by slight modifications in the experimental setup or luminophore degradation and the measurement procedure based on modulation factor requires more calibration. Figure 5 represents the RMSE in determination of oxygen concentration by use of phase-based apparent lifetimes. This figure includes the RMSE for the conventional phase-modulation method (using sine-wave signals) and the proposed multifrequency phase-modulation method (using

rectangular-wave signals), combining different harmonics. These plots show the improvement derived from use of the rectangular-wave signals as well as that derived from combination of harmonics. Compared with the sine-wave signal, the RMSE in the oxygen determination from  $\tau_\phi$  is in average 4.4 times smaller when the first harmonic is used and 7.4 times smaller when the five first harmonics are combined.

## CONCLUSIONS

From the results presented in this study, we can conclude that the use of short duty cycle rectangular signals for luminescence measuring systems based on phase-modulation luminescence spectroscopy provides (1) more complete characterization of the luminescent system and (2) improved accuracy for determining the analyte concentration.

Regarding characterization of the luminescent system, use of the proposed multifrequency phase-modulation method provides a more complete and accurate description of the system for a wide range of quencher concentrations and frequencies. It has been demonstrated that the use of several harmonics improves the accuracy in description of the frequency response with respect to the use of just one harmonic, providing an appropriate modeling of the luminescent system with a two-site model ( $R^2 > 0.9996$ ). On the other hand, the proposed method has allowed analysis of the optimal modulation frequency, which was validated with RMSE values in determination of the oxygen concentration. Even though the information used for parameter estimation for the two-sites model could have been obtained from sinusoidal excitation signals (using several frequencies subsequently), the proposed method presents the advantage of providing the information at several harmonics simultaneously from just one measurement.

It was demonstrated that the use of rectangular signals, for  $\tau_\phi$  and/or  $\tau_m$ , provides better accuracy than sinusoidal signals. This improvement is mainly associated with the use of more power for signaling (when the same luminous power is used to excite the sensing fiber). The use of a short duty cycle improves the harmonic/dc power ratio for a number of harmonics, increasing the signal-to-noise ratio at different frequencies (for a given average luminous power), which reduces the error in quantification of analyte concentration. It also allows the combination of several harmonics for determining and quantifying analyte concentration.

The combination of both analytical signals ( $\tau_\phi$  and  $\tau_m$ ) improves the accuracy provided by either  $\tau_\phi$  or  $\tau_m$  alone. The procedure proposed for combining information from different estimators has also been successfully applied to combine  $\tau_\phi$  and  $\tau_m$  information from a number of harmonics. Results show that as more information is included, the error decreases, obtaining a RMSE as low as 0.0128 at 0.5 kPa O<sub>2</sub> and 0.1532 at 20 kPa O<sub>2</sub> when  $\tau_\phi$  and  $\tau_m$  from the five first harmonics are combined. The proposed method can be easily implemented in existing photoluminescence instruments since modifications just involve the part of excitation of the light source (short duty cycle rectangular signal instead of sinusoidal signal, which usually implies a simplification of the electronics) and digital signal processing of samples after the transducer (that can be implemented in software).

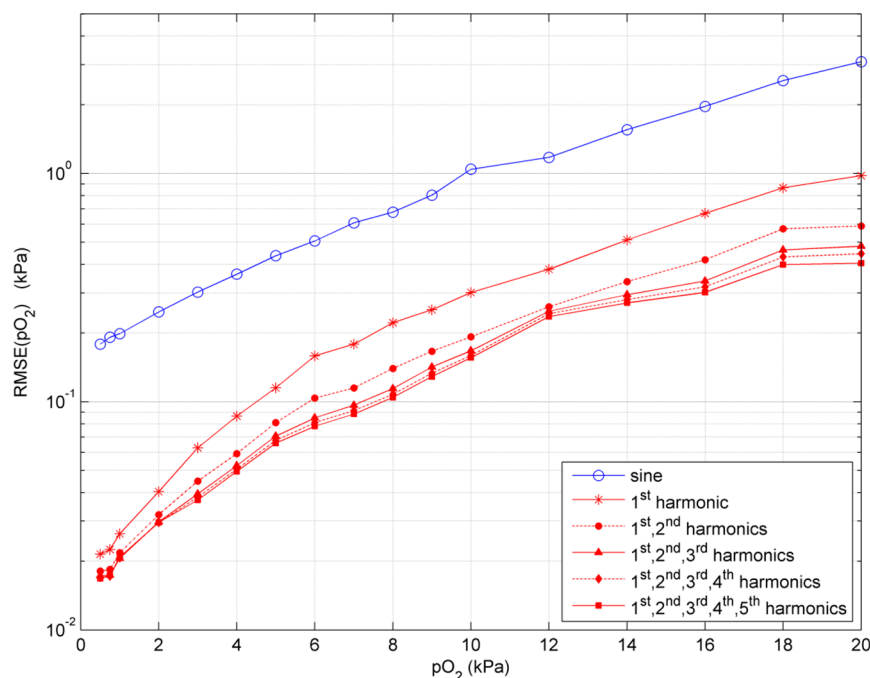


**Figure 5.** RMSE in determination of  $pO_2$  between 0.5 and 20 kPa by use of phase-based apparent lifetime with conventional phase-modulation method (blue line) and proposed multifrequency phase-modulation method (red lines) combining the  $n$  ( $n = 1, 2, \dots, 5$ ) first harmonics.

## ■ ASSOCIATED CONTENT

### Supporting Information

Additional text and equations, 14 figures, and nine tables with expressions for modeling the frequency response of a luminescent system; expressions for estimation of apparent lifetimes; procedure for combining several statistically independent measurements; pictures of optical fiber, deposited sensing film, and designed setup; examples of real signals recorded; calibration data; parameters of fitting models; and detailed experimental results. This material is available free of charge via the Internet at <http://pubs.acs.org>.

## ■ AUTHOR INFORMATION

### Corresponding Authors

\*Phone +34 958 240451; fax +34 958243328; e-mail [atv@ugr.es](mailto:atv@ugr.es).

\*E-mail [jffernan@ugr.es](mailto:jffernan@ugr.es).

### Author Contributions

The manuscript was written through contributions of all authors.

### Notes

The authors declare no competing financial interest.

## ■ ACKNOWLEDGMENTS

The authors gratefully acknowledge the financial support of the Spanish Ministry of Economy and Competitiveness (Projects CTQ2011-25316 and TEC2010-17805, and Grant BES-2009-026919 to S.M.-R.) and the Regional Government of Andalusia (Excellence projects P07-FQM-2625 and P07-FQM-2738).

## ■ REFERENCES

- (1) Lakowicz, J. R. *Principles of Fluorescence Spectroscopy*, 2nd ed.; Kluwer Academic: New York, 1999.
- (2) Medina-Rodriguez, S.; de la Torre-Vega, A.; Fernandez-Sanchez, J. F.; Fernandez-Gutierrez, A. *Sens. Actuators, B* **2013**, 176, 1110–1120.
- (3) Wang, X. D.; Wolfbeis, O. S. *Anal. Chem.* **2013**, 85, 487–508.
- (4) McGraw, C. M.; Khalil, G.; Callis, J. B. *J. Phys. Chem. C* **2008**, 112, 8079–8084.
- (5) Rowe, H. M.; Chan, S. P.; Demas, J. N.; DeGraff, B. A. *Anal. Chem.* **2002**, 74, 4821–4827.
- (6) Trettnak, W.; Kolle, C.; Reininger, F.; Dolezal, C.; O'Leary, P. *Sens. Actuators, B* **1996**, 36, 506–512.
- (7) McDonagh, C.; Kolle, C.; McEvoy, A. K.; Dowling, D. L.; Cafolla, A. A.; Cullen, S. J.; MacCraith, B. D. *Sens. Actuators, B* **2001**, 74, 124–130.
- (8) Andrzejewski, D.; Klimant, I.; Podbielska, H. *Sensors and Actuators, B: Chemical* **2002**, 84, 160–166.
- (9) Medina-Rodriguez, S.; Marín-Suarez, M.; Fernandez-Sanchez, J. F.; de la Torre-Vega, A.; Baranoff, E.; Fernandez-Gutierrez, A. *Analyst* **2013**, 138, 4607–4617.
- (10) Operating Manual and Programming Reference, SR830 DPS Lock-In Amplifier, 2.4 ed.; Stanford Research Systems: Sunnyvale, CA, June 2009.
- (11) Ergeneman, O.; Chatzipirpiridis, G.; Pokki, J.; Marín-Suarez, M.; Sotiriou, G. A.; Medina-Rodriguez, S.; Fernandez-Sanchez, J. F.; Fernandez-Gutierrez, A.; Pane, S.; Nelson, B. J. *IEEE Trans. Biomed. Eng.* **2012**, 59, 3104–3109.
- (12) Valledor, M.; Campo, J. C.; Sánchez-Barragán, I.; Costa-Fernández, J. M.; Alvarez, J. C.; Sanz-Medel, A. *Sens. Actuators, B* **2006**, 113, 249–258.
- (13) Holst, G. A.; Köster, T.; Voges, E.; Lübbers, D. W. *Sens. Actuators, B* **1995**, 29, 231–239.
- (14) O'Keeffe, G.; MacCraith, B. D.; McEvoy, A. K.; McDonagh, C. M.; McGilp, J. F. *Sens. Actuators, B* **1995**, 29, 226–230.
- (15) Masciotti, J. M.; Lasker, J. M.; Hielscher, A. H. *IEEE Trans. Instrum. Meas.* **2008**, 57, 182–189.
- (16) Langer, P.; Müller, R.; Drost, S.; Werner, T. *Sens. Actuators, B* **2002**, 82, 1–6.
- (17) Sedra, A.; Smith, K. C. *Microelectronic Circuits*, 6th ed.; Oxford University Press: London, 2009.
- (18) Marín-Suarezdel Toro, M.; Fernandez-Sanchez, J. F.; Baranoff, E.; Nazeeruddin, M. K.; Graetzel, M.; Fernandez-Gutierrez, A. *Talanta* **2010**, 82, 620–626.
- (19) Gao, F. G.; Fay, J. M.; Mathew, G.; Jeevarajan, A. S.; Anderson, M. M. *J. Biomed. Opt.* **2005**, 10, 0540051–0540056.
- (20) Philip, J.; Carlsson, K. J. *Opt. Soc. Am. A* **2003**, 20, 368–379.



- (21) Lakowicz, J. R.; Gryczynski, I.; Gryczynski, Z.; Johnson, M. L. *Anal. Biochem.* **2000**, *277*, 74–85.
- (22) Jinayim, T.; Arunrungrasmi, S.; Tanitteerapan, T.; Mungkung, N. *Int. J. Electr. Electron. Eng.* **2007**, *22*, 132–137.
- (23) Jenkins, D. M.; Zhu, C.; Su, W. W. *Appl. Eng. Agric.* **2008**, *24*, 259–263.
- (24) Li Tan, J. J. *Fundamentals of Analog and Digital Signal Processing*, 2nd ed.; AuthorHouse: Bloomington, IN, 2008.
- (25) Ogurtsov, V. I.; Papkovsky, D. B. *Sens. Actuators, B* **1998**, *51*, 377–381.
- (26) Sainz-Gonzalo, F. J.; Elosua, C.; Fernandez-Sanchez, J. F.; Popovici, C.; Fernandez, I.; Ortiz, F. L.; Arregui, F. J.; Matias, I. R.; Fernandez-Gutierrez, A. *Sens. Actuators, B* **2012**, *173*, 254–261.
- (27) Elosua, C.; Bariain, C.; Matias, I.; Rodriguez, A.; Colacio, E.; Salinas-Castillo, A.; Segura-Carretero, A.; Fernandez-Gutierrez, A. *Sensors* **2008**, *8*, 847–859.
- (28) Elosua, C.; Arregui, F. J.; Zamarreño, C. R.; Bariain, C.; Luquin, A.; Laguna, M.; Matias, I. R. *Sens. Actuators, B* **2012**, *173*, 523–529.
- (29) Schubert, E. F. *Light Emitting Diodes*, 2nd ed.; Cambridge University Press: New York, 2006.
- (30) Duda, R. O.; Hart, P. E.; Stork, D. G. *Pattern Classification*, 2nd ed.; Wiley: New York, 2000.
- (31) Demas, J. N.; DeGraff, B. A. *Sens. Actuators, B* **1993**, *11*, 35–41.